

Research Article

Organic Photovoltaic Cells Based on PbPc Nanocolumns Prepared by Glancing Angle Deposition

Yang Liu, Fujun Zhang, and Jian Wang

Key Laboratory of Luminescence and Optical Information, Ministry of Education, Beijing Jiaotong University, Beijing 100044, China

Correspondence should be addressed to Fujun Zhang; fjzhang@bjtu.edu.cn

Received 24 January 2013; Accepted 14 March 2013

Academic Editor: Sudhakar Shet

Copyright © 2013 Yang Liu et al. This is an open access article distributed under the Creative Commons Attribution License, which permits unrestricted use, distribution, and reproduction in any medium, provided the original work is properly cited.

Organic small material lead phthalocyanine (PbPc) nanocolumns were prepared via glancing angle deposition (GLAD) on indium tin oxide (ITO) coated glass substrates. Organic electron acceptor materials fullerene (C_{60}) was evaporated onto the nanocolumn PbPc thin films to prepare heterojunction structure ITO/PbPc/ C_{60} /Bphen/Al organic photovoltaic cells (OPVs). It is worthwhile to mention that C_{60} molecules firstly fill the voids between PbPc nanocolumns and then form impact C_{60} layer. The interpenetrating electron donor/acceptor structure effectively enhances interface between electron donor and electron acceptor, which is beneficial to exciton dissociation. The short circuit current density (J_{sc}) of organic photovoltaic devices (OPVs) based on PbPc nanocolumn was increased from 1.19 mA/cm^2 to 1.74 mA/cm^2 , which should be attributed to the increase of interface between donor and acceptor. The effect of illumination intensity on the performance of OPVs was investigated by controlling the distance between light source and sample, and the J_{sc} of two kind of OPVs was increased along with the increase of illumination intensity.

1. Introduction

Organic photovoltaic devices (OPVs) are potential candidates for light weight, low-cost solar energy conversion, and ease of processing [1–4]. Typical OPVs are composed of a donor (p-type semiconductor) and an acceptor (n-type semiconductor) as active layers. Photo-generated excitons are dissociated into free holes and electrons at the interface of donor-acceptor, the free charge carriers are collected by the electrodes, respectively. Two kinds of architectures with this D-A interface were developed: planar heterojunction (PHJ) and bulk heterojunction (BHJ) [5, 6]. Tang firstly reported PHJ devices based on CuPc/ C_{60} as the active layer, which was considered as a milestone of OPVs development [7]. The efficiency of exciton dissociation of the PHJ cell is decreased due to the limit of the D-A interface. Some photo-generated excitons in the active layers maybe quenched when travelling a distance longer than the diffusion length to the D-A interface. The exciton dissociation efficiency could be increased in the BHJ cells, where the donor and acceptor form an interpenetrating network of structures which shortens the excitons' route to the D-A interface. However, random distribution of donor and acceptor materials in the blend

film may lead to lower charge collection due to the so-called dead ends in the conducting paths and long conducting distance from the active layers to the electrodes [4, 8]. Therefore, the key point to enhance the PCE is to form the structure which provides high interface area and good charge transport routes in the active layer. Knorr and Hoffman firstly discovered a new kind of evaporation technology, named as glancing angle deposition (GLAD). The morphology and microstructure of this kind of films prepared by GLAD could be easily controlled by changing the substrate rotating speed, the evaporation speed, the distance between substrate and evaporation source, the angle between incoming incidence flux, and the substrate surface [9–13]. Van Dijken et al. applied the GLAD technology to fabricate donor layer and then spin-coated acceptor solution onto the nanostructure donor layer for achieving a mixed heterojunction OPVs, which shows a better performance than the common bilayer heterojunction OPV [14–16]. Also this approach has been used to fabricate nanocolumn structural thin films for indium tin oxide (ITO) electrodes [17] and electron acceptor material C_{60} [18, 19], providing large interfacial area for exciton extraction and charge carrier collection. Hoppe et al. pointed out that only

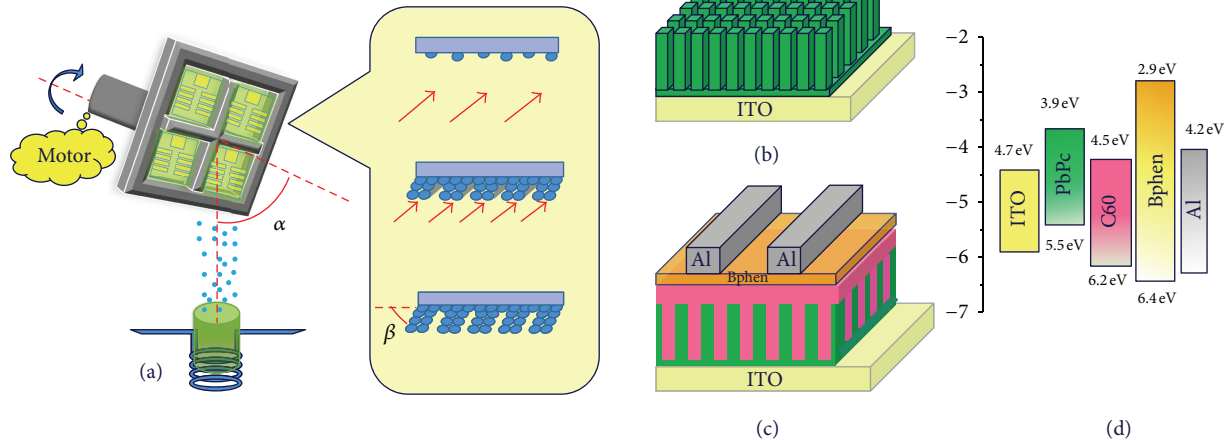


FIGURE 1: (a) Schematic diagram of GLAD installation, (b) schematic diagram of PbPc nanocolumn, (c) schematic OPV device architecture (ITO/PbPc/C₆₀/Bphen/Al), and (d) energy level configuration of the used materials.

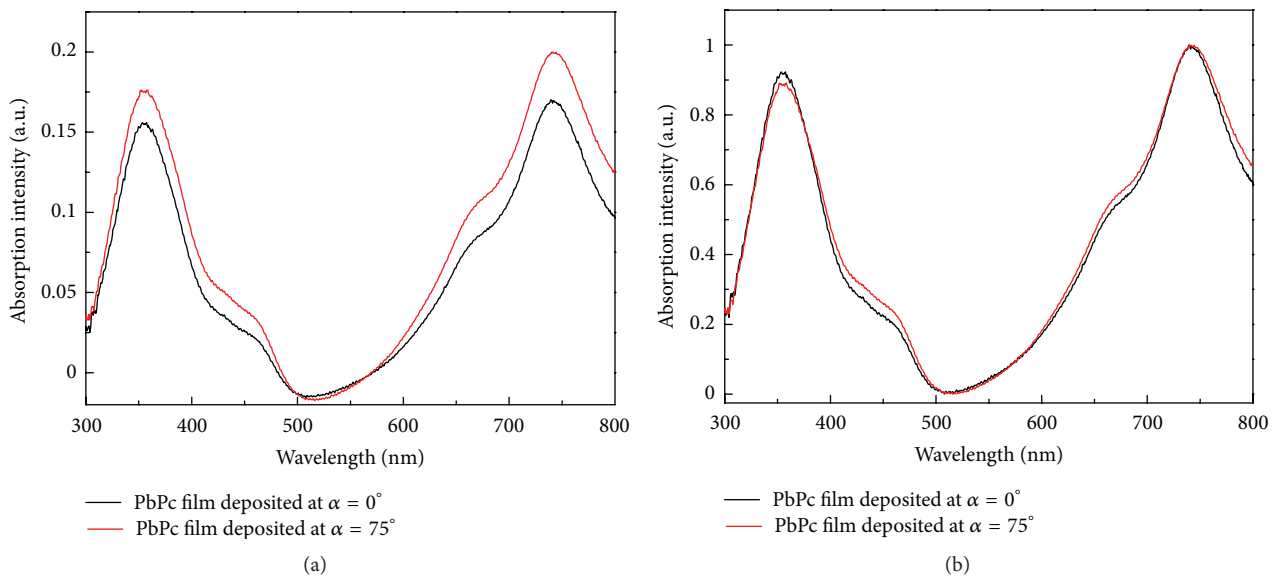


FIGURE 2: (a) The absorption spectra of PbPc films prepared by normal conditions and glancing angle deposition at 75°, (b) the normalized absorption spectra.

30% of the photons in the whole solar spectrum have energy higher than 1.9 eV [20]. Lead phthalocyanine (PbPc), as a promising small molecule donor material, has attracted more and more attention due to its near infrared absorption [21]. Organic electron acceptor materials fullerene (C₆₀) is a proper matching for PbPc to form the heterojunction.

In this paper, two kinds of OPVs with different morphology PbPc films as the donor layer and C₆₀ films as the acceptor layer were fabricated and measured under different illumination intensities. The OPVs with PbPc films prepared by GLAD show better performance compared with the OPVs based on PbPc films prepared under normal conditions. The underlying reason for the improvement of OPVs performance was discussed from the effect of PbPc film morphology on the absorption spectra and donor/acceptor interfaces.

2. Experimental Details

Indium tin oxide (ITO) coated glass substrates with a sheet resistance of 15 Ω/□ (purchased from Shenzhen Jinghua Displays Co. Ltd.) were cleaned with detergent, deionized water and ethanol successively in ultrasonic baths for 15 min. All substrates were dried by nitrogen gas and were treated by UV-ozone for 10 min to improve the work function of ITO. Electron donor material PbPc (purchased from Jilin Optical and Electronic Materials Co., Ltd.) was deposited on the ITO substrates via GLAD. A computer-controlled stepper motor was used to control rotation of substrate about the substrate surface normal. The angle between the molecular flux incidence and the substrate normal was set to 75° and 0°. The substrate rotation rate was controlled about 6

rounds per minute (rpm). The deposition rate was about 0.1 ~ 0.3 nm/s, which was monitored by quartz-crystal oscillator monitor. Electron acceptor material C_{60} (purchased from Alfa Aesar) films and hole blocking material 4,7-diphenyl-1, 10-phenanthroline (Bphen, purchased from Jilin OLED Material Tech Co., Ltd) films were deposited by thermal evaporation under 4×10^{-4} Pa vacuum conditions successively. Al cathode of 100 nm thickness was thermally evaporated on the hole blocking layer through shadow masks. The active area of the cells was 3×3 mm². The schematic diagram of GLAD installation is shown in Figure 1(a) (left side): the angle between substrate normal and the incoming particle flux is defined as α , and the angle between PbPc nanocolumns and substrate surface normal is defined as β . The schematic process of GLAD is presented in Figure 1(a) (right side): (i) a few PbPc particles arrive at the substrate at first and form some islands on the surface, (ii) the former islands block the incoming particles resulting in selective growth along the island due to the shadow effect, (iii) formed column structure. The schematic diagram of PbPc nanocolumn films and OPVs are shown in Figures 1(b) and 1(c). The energy level alignment of used materials is shown in Figure 1(d).

Morphology of PbPc films was investigated by a Hitachi S-4800 scanning electron microscope (SEM) with a secondary electron detector. The absorption spectra of films were measured via Shimadzu UV-3101PC UV-VIS. Current-voltage (I - V) curves of fabricated OPVs were measured by Keithley 4200 source measure unit under 100 mW/cm² illumination or dark conditions.

3. Results and Discussions

The absorption spectra of PbPc films under different preparation conditions were measured and are shown in Figure 2(a). The absorption spectrum of PbPc film prepared under normal conditions (titled angle is 0°) shows two broader absorption peaks, one at around 515 nm and the other at 350 nm, which accords with previously observed results [22]. The absorption spectrum of PbPc thin films prepared by GLAD with the tilted angle 75° is similar with that of PbPc thin film prepared under normal conditions. In order to investigate the effect of film prepared conditions on its absorption performance, the normalized absorption spectra are shown in Figure 2(b). It is worthwhile to mention that PbPc thin films prepared by GLAD have slightly strong absorption from 400 nm to 480 nm, comparing with that of PbPc films prepared under normal conditions, which should be attributed to the increased J_{sc} of OPVs (as shown in Figure 3).

Two kinds of bilayer heterojunction OPVs with different structural PbPc films as the electron donor layers were prepared, Cells A: ITO/PbPc (40 nm, prepared under normal conditions)/ C_{60} (50 nm)/Bphen (8 nm)/Al (100 nm), Cells B: ITO/PbPc (40 nm, prepared by GLAD)/ C_{60} (50 nm)/Bphen (8 nm)/Al (100 nm). The 8 nm Bphen layer was used as hole-blocking layer and protection layer for the active layer during metal deposition. The J - V characteristics of two kinds of OPVs were measured at 100 mW/m² illumination and in dark conditions, as shown in Figure 3. The J_{sc} of Cells B is

TABLE 1: Key parameters of two kinds of OPVs under 100 mW/cm² illumination intensity.

	J_{sc} (mA/cm ²)	V_{oc} (V)	FF (%)	PCE (%)
Cells A	1.19	0.40	35.4	0.16
Cells B	1.74	0.34	35.95	0.21

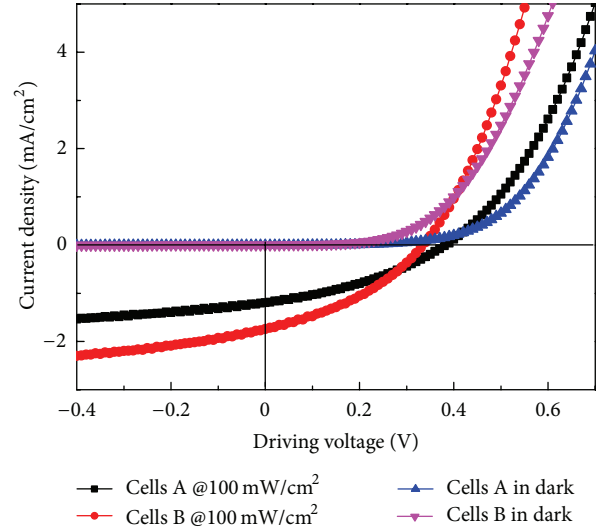


FIGURE 3: J - V characteristics of two kinds of OPVs under 100 mW/cm² illumination intensity and in dark conditions.

about 1.5 times larger than that of Cells A, which may be attributed to the increase of absorption and donor/acceptor interface induced by PbPc nanocolumn structure prepared by GLAD. The open-circuit voltage (V_{oc}) of the Cells B is about 0.34 V and lower than that (0.4 V) of Cells A, which may be induced by the leakage current of Cells B resulting from the interface between PbPc layer and ITO. According to the dark J - V characteristics curves of two kinds of cells, it is apparent that both kinds of cells have good blocking characteristics in the reverse bias region, the Cells B have a lower break-over voltage in forward bias region. The power conversion efficiency (PCE) of Cells B is about 0.21%, which is larger than that (0.16%) of Cells A. The key parameters, including V_{oc} , J_{sc} , FF and PCE of the two kinds of OPV cells are summarized in Table 1.

In order to further investigate the effect of PbPc film morphology on the performance of OPVs, the J - V characteristic curves were measured under different illumination intensities. Figure 4(a) shows the J - V characteristic curves of Cells A; Figure 4(b) shows the J - V characteristic curves of Cells B. Both kinds of OPVs also show similar behaviors dependent on the illumination intensity. The J_{sc} is increased along with the increase of illumination intensity, and V_{oc} keeps constant under different illumination intensities. It is known that photogenerated excitons strongly depend on the incident photon numbers, which have enough energy to excite active layer materials [23, 24]. The increased J_{sc} should be well understood due to more photo-generated excitons under higher illumination intensity. It is known that V_{oc} is

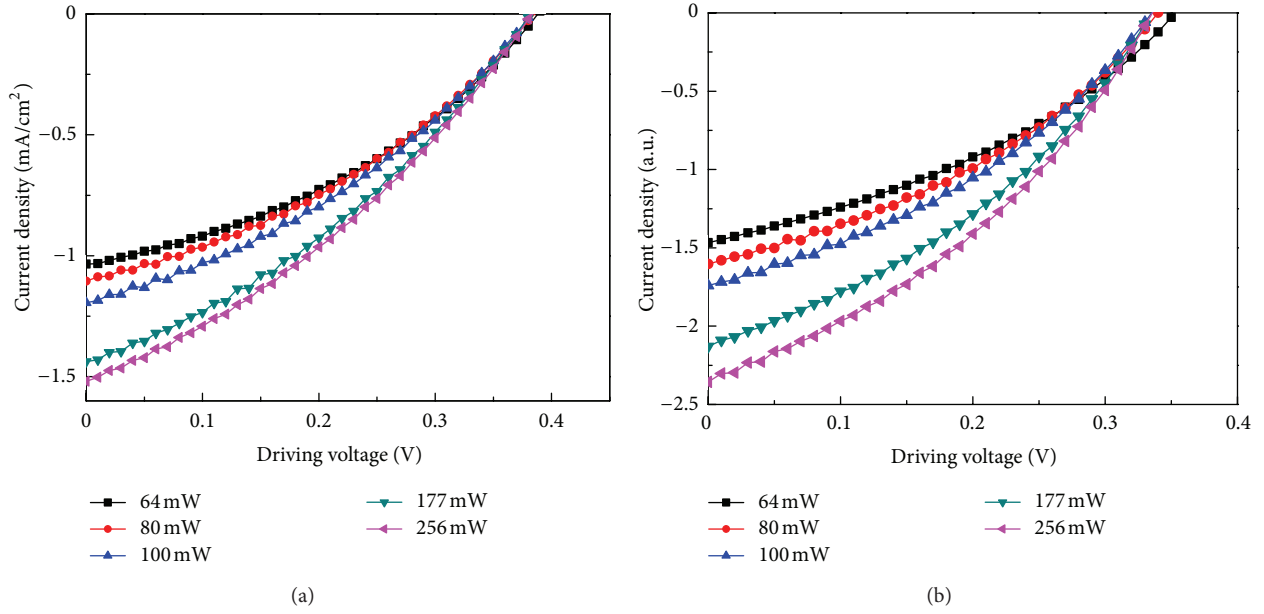


FIGURE 4: J - V characteristics of two kinds of OPVs under different illumination intensities, (a) PbPc films prepared under normal conditions; (b) PbPc films prepared by GLAD.

TABLE 2: OPVs parameters of Cells A prepared under normal condition under different illumination intensities.

Input power	J_{sc} (mA/cm ²)	V_{oc} (V)	FF (%)	PCE (%)
64 mW	1.03	0.4	37.6	0.23
80 mW	1.11	0.4	35.8	0.19
100 mW	1.19	0.4	35.4	0.16
177 mW	1.44	0.4	34.1	0.11
256 mW	1.52	0.4	33.5	0.08

determined by the difference between the highest occupied molecular orbital (HOMO) of the donor and the lowest unoccupied molecular orbital (LUMO) of the acceptor [25]. However, the large input power also increases the active layer temperature, which may induce exciton quenched in organic materials [26]. The exciton dissociation and quenching are two competitive processes, which codetermine PCE of OPVs. According to the data summarized in Tables 2 and 3, the PCE of OPVs is decreased along with the increase of illumination intensity. It means that more photo-generated excitons were quenched under higher illumination intensity, which results in the decrease of PCE. The key parameters of two kinds of OPVs are summarized in Tables 2 and 3.

From the variation of two kinds of cells' photovoltaic characteristic of OPVs, PbPc films prepared by GLAD have a positive effect on the performance of OPVs. In order to clarify the positive effect, the morphology of PbPc films prepared by normal conditions and GLAD were investigated by SEM, as shown in Figure 5. From the SEM images of Figures 5(a) and 5(b), the surface of PbPc films prepared by GLAD shows some small holes, and PbPc films prepared

TABLE 3: OPVs parameters of Cells B prepared by GLAD under different illumination intensities.

Input power	J_{sc} (mA/cm ²)	V_{oc} (V)	FF (%)	PCE (%)
64 mW	1.47	0.35	36.40	0.30
80 mW	1.60	0.34	36.34	0.25
100 mW	1.74	0.34	35.95	0.21
177 mW	2.13	0.34	35.69	0.15
256 mW	2.36	0.34	35.34	0.11

under normal conditions look more smooth. According to Figures 5(c) and 5(d), the surface roughness of PbPc films prepared by GLAD should be larger than that of PbPc films prepared by normal condition. The similar experimental phenomenon was observed in our pervious experimental results [27, 28]. The dynamic growth process of PbPc films is described by shadow effect and atomic surface diffusion. Shadow effect implies that one given point on the surface can receive fewer particles than other points, because nearby surface features block some of the incoming particles, which results in tilted nanocolumns on the substrates [29]. Atomic scale fluctuations inevitably exist on the nominally smooth surfaces. PbPc particles arrive at the top of the surface and will migrate to other points due to their kinetic energy, leading to a smooth surface. The competition between these two factors strongly determines the morphological evolution of the growing surface. The schematic growth process is shown in Figure 1(b).

During the glancing angle deposition process, the angle (β) between PbPc nanocolumns and substrate surface normal strongly depends on the angle (α) between substrate surface normal and the incoming particle flux. The angle β is not simply proportional to the cosine of the tilted angle α , which

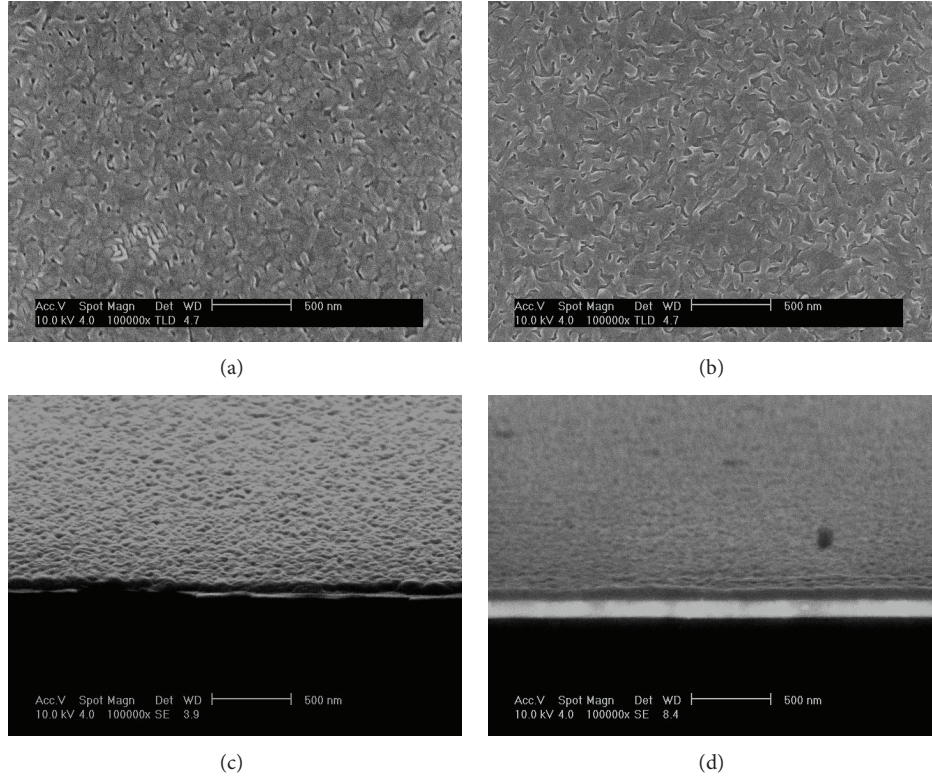


FIGURE 5: (a) SEM images of PbPc films prepared by GLAD at $\alpha = 75^\circ$, (b) SEM images of PbPc films prepared under normal conditions, (c) the side views of PbPc films prepared by GLAD at $\alpha = 75^\circ$, (d) the side views of PbPc films prepared under normal conditions.

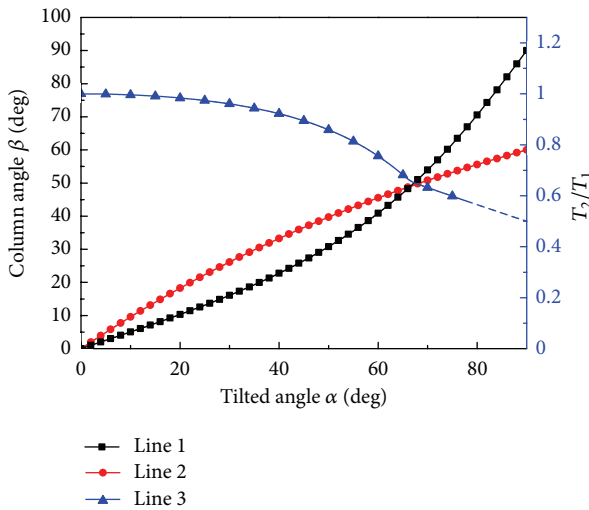


FIGURE 6: The relationship between column angle and the tilted angle, the blue line shows the ratio of actual film thickness to the thickness monitored by quartz-crystal oscillator monitor.

is given by the following formulas: (i) tangent rule ($\tan \beta = 0.5 \tan \alpha$, $\alpha < 70^\circ$) described by line 1 in Figure 6 and (ii) cosine rule ($2 \sin(\alpha - \beta) = 1 - \cos \alpha$, $\alpha > 70^\circ$), described by line 2 in Figure 6 [30]. In this work, α was set to 75° , therefore column angle β was measured by formula

(II) resulting in 45° . In terms of the thickness of PbPc film, the actual thickness of PbPc film is defined as T_1 , and the evaporation thickness monitored by quartz-crystal oscillator monitor is T_2 . The relationship of the two parameters could be expressed as $T_1 = T_2 \cos \beta$, described by line 3 in Figure 6. In the Cells A, the thicknesses of the PbPc films prepared under normal conditions are 40 nm. For keeping PbPc films thickness constant in the two kinds of Cells, the evaporation thickness (T_2) monitored by quartz-crystal oscillator monitor was controlled about 56.5 nm, which could keep the factual PbPc films thickness (T_1) at 40 nm. The PbPc films prepared by GLAD show nanocolumn structures, which could increase the interfaces with C_{60} , resulting in more exciton dissociation. The PbPc nanocolumn also provides an effective charge carrier transporting road, which is beneficial to the charge carrier collection by their individual cathodes.

4. Conclusion

Two kinds of OPVs based on different morphology PbPc film prepared under normal conditions or glancing angle deposition were fabricated; the OPVs based on PbPc nanocolumn prepared by GLAD obtain a larger PCE compared with OPVs based on PbPc film prepared under normal conditions. The main contribution for the increase of PCE should be due to the enhanced absorption and enlarger interface between PbPc and C_{60} layer. The effect of illumination intensity on the performance of OPVs was investigated by controlling the

distance between light source and sample, the J_{sc} of two kind of OPVs was increased along with the increase of illumination intensity.

Acknowledgments

The authors express their thanks to the Beijing Natural Science Foundation (2122050) and Basic Research Foundation of the Central Universities (2013JBZ004). The authors also thank the supports on using synchrotron radiation light from the Beijing Synchrotron Radiation Facility. F. J. Zhang thanks the support from the State Key Laboratory of Catalysis and the Key Laboratory of Photochemical Conversion and Optoelectronic Materials, TIPC, CAS.

References

- [1] H. Y. Chen, J. Hou, S. Zhang et al., "Polymer solar cells with enhanced open-circuit voltage and efficiency," *Nature Photonics*, vol. 3, no. 11, pp. 649–653, 2009.
- [2] Y. K. Jin, K. Lee, N. E. Coates et al., "Efficient tandem polymer solar cells fabricated by all-solution processing," *Science*, vol. 317, no. 5835, pp. 222–225, 2007.
- [3] T. D. Nielsen, C. Cruickshank, S. Foged, J. Thorsen, and F. C. Krebs, "Business, market and intellectual property analysis of polymer solar cells," *Solar Energy Materials and Solar Cells*, vol. 94, no. 10, pp. 1553–1571, 2010.
- [4] F. Yang, M. Shtein, and S. R. Forrest, "Controlled growth of a molecular bulk heterojunction photovoltaic cell," *Nature Materials*, vol. 4, no. 1, pp. 37–41, 2005.
- [5] F. J. Zhang, X. W. Xu, W. H. Tang et al., "Recent development of the inverted configuration organic solar cells," *Solar Energy Materials and Solar Cells*, vol. 95, no. 7, pp. 1785–1799, 2011.
- [6] Z. L. Zhuo, F. J. Zhang, J. Wang et al., "Efficiency improvement of polymer solar cells by iodine doping," *Solid-State Electronics*, vol. 63, pp. 83–88, 2011.
- [7] C. W. Tang, "Two-layer organic photovoltaic cell," *Applied Physics Letters*, vol. 48, no. 2, pp. 183–185, 1986.
- [8] S. Yu, C. Klimm, P. Schäfer, J. P. Rabe, B. Rech, and N. Koch, "Organic photovoltaic cells with interdigitated structures based on pentacene nanocolumn arrays," *Organic Electronics*, vol. 12, no. 12, pp. 2180–2184, 2011.
- [9] T. G. Knorr and R. W. Hoffman, "Dependence of geometric magnetic anisotropy in thin iron films," *Physical Review*, vol. 113, no. 4, pp. 1039–1046, 1959.
- [10] M. O. Jensen and M. J. Brett, "Porosity engineering in glancing angle deposition thin films," *Applied Physics A*, vol. 80, no. 4, pp. 763–768, 2005.
- [11] M. M. Hawkeye and M. J. Brett, "Glancing angle deposition: fabrication, properties, and applications of micro- and nanostructured thin films," *Journal of Vacuum Science and Technology A*, vol. 25, no. 5, pp. 1317–1335, 2007.
- [12] K. Robbie and M. J. Brett, "Sculptured thin films and glancing angle deposition: growth mechanics and applications," *Journal of Vacuum Science and Technology A*, vol. 15, no. 3, pp. 1460–1465, 1997.
- [13] K. Robbie, M. J. Brett, and A. Lakhtakia, "Chiral sculptured thin films," *Nature*, vol. 384, p. 616, 1996.
- [14] J. van Dijken, M. Fleischauer, and M. J. Brett, "Morphology control of CuPc thin films using Glancing Angle Deposition," in *Proceedings of the 33rd IEEE Photovoltaic Specialists Conference (PVSC '08)*, pp. 1–4, IEEE, 2008.
- [15] J. G. van Dijken, M. D. Fleischauer, and M. J. Brett, "Controlled nanostructuring of CuPc thin films via glancing angle deposition for idealized organic photovoltaic architectures," *Journal of Materials Chemistry*, vol. 21, no. 4, pp. 1013–1019, 2011.
- [16] J. G. van Dijken, M. D. Fleischauer, and M. J. Brett, "Solvent effects on ZnPc thin films and their role in fabrication of nanostructured organic solar cells," *Organic Electronics*, vol. 12, no. 12, pp. 2111–2119, 2011.
- [17] D. A. Rider, R. T. Tucker, B. J. Worfolk et al., "Indium tin oxide nanopillar electrodes in polymer/fullerene solar cells," *Nanotechnology*, vol. 22, no. 8, Article ID 085706, 2011.
- [18] M. Thomas, W. Li, Z. S. Bo, and M. J. Brett, "Inverted photovoltaic cells of nanocolumnar C₆₀ filled with solution processed small molecule 3-Q," *Organic Electronics*, vol. 13, no. 11, pp. 2647–2652, 2012.
- [19] M. Thomas, B. J. Worfolk, D. A. Rider, M. T. Taschuk, J. M. Buriak, and M. J. Brett, "C₆₀ fullerene nanocolumns-polythiophene heterojunctions for inverted organic photovoltaic cells," *ACS Applied Materials & Interfaces*, vol. 3, no. 6, pp. 1887–1894, 2011.
- [20] H. Hoppe, M. Niggemann, C. Winder et al., "Nanoscale morphology of conjugated polymer/fullerene-based bulk-heterojunction solar cells," *Advanced Functional Materials*, vol. 14, no. 10, pp. 1005–1011, 2004.
- [21] H. S. Shim, H. J. Kim, J. W. Kim et al., "Enhancement of near-infrared absorption with high fill factor in lead phthalocyanine-based organic solar cells," *Journal of Materials Chemistry*, vol. 22, pp. 9077–9081, 2012.
- [22] W. Zhao, "Enhancing photovoltaic response of organic solar cells using a crystalline molecular template," *Organic Electronics*, vol. 13, no. 1, pp. 129–135, 2012.
- [23] P. Kumar, S. C. Jain, H. Kumar, S. Chand, and V. Kumar, "Effect of illumination intensity and temperature on open circuit voltage in organic solar cells," *Applied Physics Letters*, vol. 94, no. 18, Article ID 183505, 3 pages, 2009.
- [24] F. J. Zhang, F. Y. Sun, Y. Z. Shi et al., "Effect of an ultra-thin molybdenum trioxide layer and illumination intensity on the performance of organic photovoltaic devices," *Energy and Fuels*, vol. 24, no. 7, pp. 3739–3742, 2010.
- [25] C. J. Brabec, A. Cravino, D. Meissner et al., "The influence of materials work function on the open circuit voltage of plastic solar cells," *Thin Solid Films*, vol. 403–404, pp. 368–372, 2002.
- [26] V. Podzorov, E. Menard, J. A. Rogers, and M. E. Gershenson, "Hall effect in the accumulation layers on the surface of organic semiconductors," *Physical Review Letters*, vol. 95, no. 22, Article ID 226601, pp. 1–4, 2005.
- [27] L. F. Lu, Z. Xu, F. J. Zhang et al., "Preparation and transmissivity of ZnS nanocolumn thin films with glancing angle deposition technology," *Spectroscopy and Spectral Analysis*, vol. 30, no. 2, pp. 504–507, 2010.
- [28] L. F. Lu, Z. Xu, F. J. Zhang et al., "Using ZnS nanostructured thin films to enhance light extraction from organic light-emitting diodes," *Energy and Fuels*, vol. 24, no. 7, pp. 3743–3747, 2010.
- [29] A. Amassian, K. Kaminska, M. Suzuki, L. Martinu, and K. Robbie, "Onset of shadowing-dominated growth in glancing angle deposition," *Applied Physics Letters*, vol. 91, no. 17, Article ID 173114, 3 pages, 2007.
- [30] X. Xiao, G. Dong, C. Xu et al., "Structure and optical properties of Nb₂O₅ sculptured thin films by glancing angle deposition," *Applied Surface Science*, vol. 255, no. 5, pp. 2192–2195, 2008.



Hindawi

Submit your manuscripts at
<http://www.hindawi.com>

